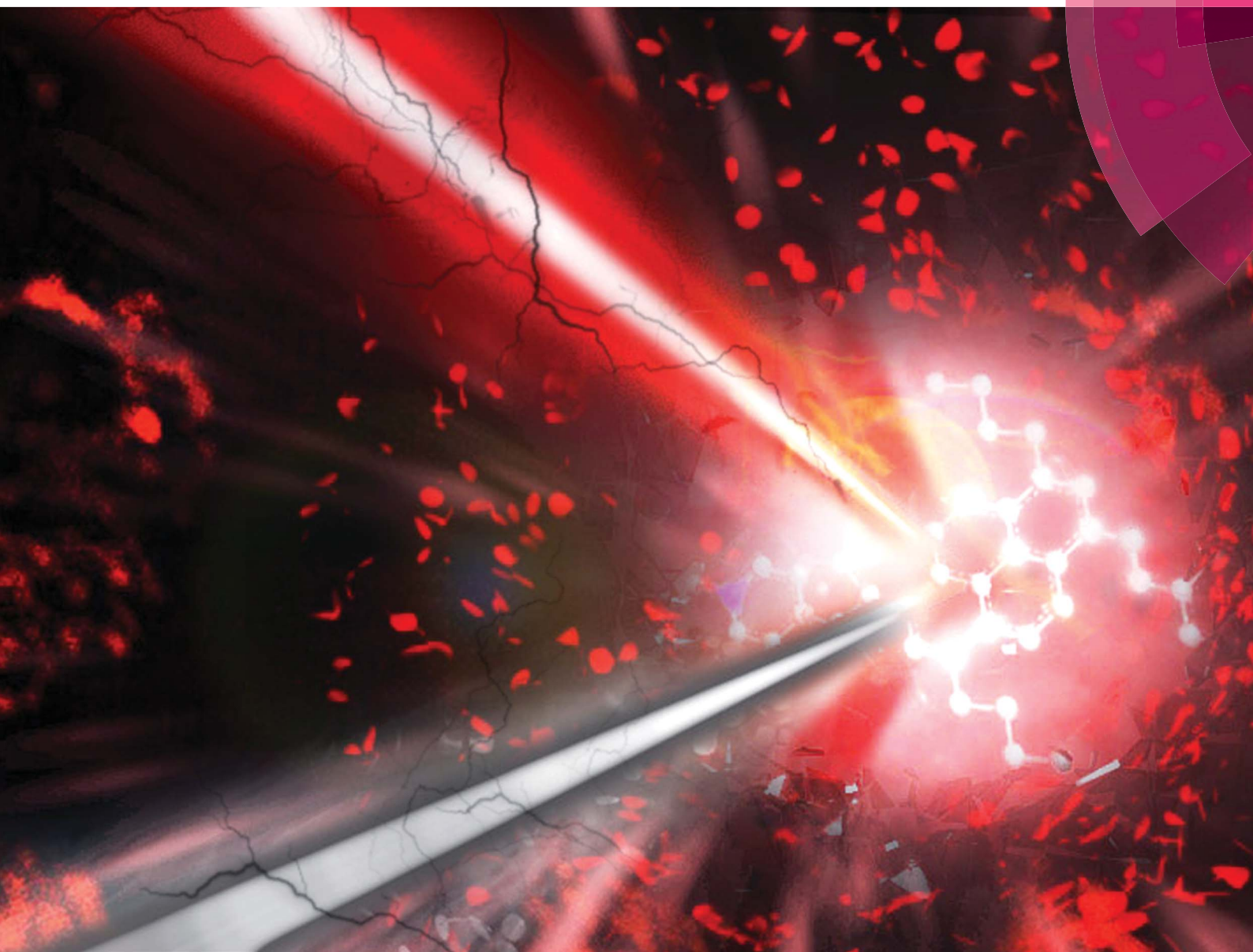


# Journal of Materials Chemistry B

Materials for biology and medicine

[www.rsc.org/MaterialsB](http://www.rsc.org/MaterialsB)



ISSN 2050-750X



## PAPER

Jun Kawamata, Gen-ichi Konishi *et al.*

A novel pyrene-based two-photon active fluorescent dye efficiently excited and emitting in the 'tissue optical window (650–1100 nm)'

CrossMark  
click for updatesCite this: *J. Mater. Chem. B*, 2015, 3, 184

## A novel pyrene-based two-photon active fluorescent dye efficiently excited and emitting in the 'tissue optical window (650–1100 nm)'†

Yosuke Niko,<sup>a</sup> Hiroki Moritomo,<sup>b</sup> Hiroyuki Sugihara,<sup>c</sup> Yasutaka Suzuki,<sup>b</sup> Jun Kawamata<sup>\*b</sup> and Gen-ichi Konishi<sup>\*ad</sup>

The development of two-photon (TP) active fluorophores remains an important issue. Dyes that can be excited and fluoresce efficiently in the 'tissue optical window' (650–1100 nm) are especially in demand to maximize the underlying performance of two-photon fluorescence microscopy (TPFM) as an advanced optical technique. Ideally, such dyes would be compatible with the 1050 nm femtosecond fibre laser, which has recently been developed as an inexpensive excitation source to make the TPFM technique universal. In this work, we designed and synthesized a novel pyrene-based acceptor– $\pi$ –acceptor (A– $\pi$ –A) dye, **PY**, which exhibited outstanding properties such as bright fluorescence ( $\lambda_{\text{em}} = 650$  nm and  $\Phi_{\text{FL}} = 0.80$ ) and a large two-photon absorption cross-section (1100 GM (1 GM =  $10^{-50}$  cm<sup>4</sup> per photon per molecule) at 950 nm and 380 GM at 1050 nm) in the tissue optical window. In living mitochondria, **PY** provided more sensitive microscopic images than current dyes and showed great potential to be a building block of TP active fluorescent probes for the 1050 nm fibre laser. We believe that the exceptional properties of **PY** will be extended to other fluorescent probes through further chemical modification.

Received 23rd August 2014  
Accepted 17th October 2014

DOI: 10.1039/c4tb01404a

www.rsc.org/MaterialsB

## Introduction

Two-photon fluorescence microscopy (TPFM) has received considerable attention as an advanced optical technique, especially in the biomedical field, because it can provide both *in vivo* and *in vitro* three-dimensional (3D) images deep within the samples of interest using low-energy photons, which significantly reduces the photodamage and photobleaching of tissues and organs.<sup>1–4</sup> The usability of this technique strongly depends on the performance of the probe molecules; therefore, the development of two-photon (TP) activatable fluorophores remains an urgent issue. In recent years, remarkable progress has been made in the molecular design concepts for dyes to be used in practical applications.<sup>1,2,5,6</sup> For instance, TP active dyes that function as detectors of chemical or biological events in the target system and can realize ratiometric imaging are highly important.<sup>5,6</sup> The significance of this type of function is

apparent from the substantial amount of research on the use of one-photon activatable molecular probes.<sup>7,8</sup>

The attractive, but still challenging feature of TP active dyes is their efficient TP absorption and bright fluorescence bands in the 650–1100 nm region.<sup>5</sup> This wavelength region is the so-called 'tissue optical window', where undesired absorption of excitation light and fluorescence, light scattering, and autofluorescence due to biological media are minimal.<sup>4</sup> However, the development of such dyes has been limited,<sup>6,7</sup> as seen from current reviews.<sup>1,2</sup> Furthermore, TP dyes would ideally be excited with the 1050 nm femtosecond fibre laser, which has recently been developed as an inexpensive excitation source.<sup>9</sup> One of the advantages of fluorescence techniques is that they are relatively cheaper than other diagnostic tools like single-photon emission computed tomography (SPECT).<sup>10</sup> Considering the expensive hardware used, this is currently not the case for TPFM; however, the compatibility of TP dyes with such a fibre laser would make TPFM universally available. The inherent advantages of the TPFM technique would be truly maximized by employing probes that satisfy all the above mentioned requirements.

To this end, we have developed a novel pyrene-based acceptor– $\pi$ –acceptor (A– $\pi$ –A) dye based on the following rationale. Our group has previously exploited a molecular design strategy to construct A– $\pi$ –A structures (*i.e.* fluorene-based **FLW**, naphthalene-based **NP**, and anthracene-based **AC**, shown in Fig. 1) for TPFM.<sup>5c</sup> In these structures, two pyridinium moieties,

<sup>a</sup>Department of Organic and Polymeric Materials, Tokyo Institute of Technology, 2-12-1, Ookayama, Tokyo 152-8552, Japan. E-mail: konishi.g.aa@m.titech.ac.jp; j-kawa@yamaguchi-u.ac.jp

<sup>b</sup>Graduate School of Medicine, Yamaguchi University, 1677-1, Yoshida, Yamaguchi 753-8512, Japan

<sup>c</sup>Graduate School of Science and Engineering, Yamaguchi University, 1677-1, Yoshida, Yamaguchi 753-8512, Japan

<sup>d</sup>PRESTO, Japan Science and Technology Agency (JST), Japan

† Electronic supplementary information (ESI) available. See DOI: 10.1039/c4tb01404a



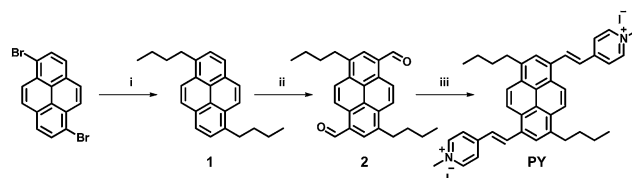
acting as electron acceptors (A), were linked by vinyl linkers to a  $\pi$ -centre consisting of a planar and rigid aromatic chromophore, typified by polycyclic aromatic hydrocarbons (PAHs). The dyes comprising such structures exhibited large TP absorption cross-sections ( $\sigma^{(2)}$ ) at longer wavelengths owing to strong intramolecular charge transfer characteristics and extended  $\pi$ -conjugation lengths. However, the PAH-based A- $\pi$ -A dyes we have developed so far do not satisfy the above-mentioned performance characteristics. Herein, we focused on the pyrene chromophore as a new  $\pi$ -centre for A- $\pi$ -A dyes. Pyrene often has several photophysical and structural advantages when compared with the other PAHs, *e.g.* longer excitation and emission wavelengths, higher fluorescence quantum yields ( $\Phi_{\text{FL}}$ ), higher absorption extinction coefficients ( $\epsilon$ ), more  $\pi$ -electrons, and greater planarity and symmetry.<sup>11,12</sup> These properties are thought to be related to the spectral red shift of fluorescence and TP absorption and the enhancement of  $\sigma^{(2)}$  values.<sup>1</sup>

In this paper, we report the synthesis of a pyrene-based A- $\pi$ -A dye **PY** [[4,4'-((1*E*,1'*E*)-(3,8-dibutylpyrene-1,6-diyl)bis(ethene-2,1-diyl))bis(1-methylpyridin-1-ium) iodide]] and its outstanding optical properties in dimethylsulfoxide (DMSO). We also show the actual performance of **PY** in mitochondrial imaging using the TPFM technique and compare its performance with those of **FLW**, **NP**, **AC**, commercially available dyes, and other existing TP activatable dyes. These results demonstrated that **PY** is applicable in biological applications, and its use could be extended to other organic diagnostic tools, like fluorescent nanoparticles,<sup>13</sup> through further structural modification.

## Results and discussion

### Synthesis of PY

The synthetic protocol of **PY** is outlined in Scheme 1. Firstly, compound **1** was prepared through the introduction of two *n*-butyl groups into the 3 and 8 positions of pyrene. Next, Friedel-Crafts formylation was conducted to obtain a diformylated compound **2**. Finally, Knoevenagel condensation between **2** and 1,4-dimethylpyridin-1-ium iodide was carried out to afford the final product **PY**. The role of the *n*-butyl groups was to enhance the solubility for the easier preparation of compound **2** and to fix the two formyl groups at the 1 and 6 positions. This pattern



**Scheme 1** Synthetic route to **PY**. (i) (1) THF, *n*-BuLi, 1-bromobutane, 0 °C, 12 h (2) *n*-C<sub>4</sub>H<sub>9</sub>, r.t., 3 h (78%). (ii) CH<sub>2</sub>Cl<sub>2</sub>, TiCl<sub>4</sub>, Cl<sub>2</sub>CHOCH<sub>3</sub>, 0 °C, 23 h (41%). (iii) MeOH/CHCl<sub>3</sub>, piperidine, 1,4-dimethylpyridin-1-ium iodide, reflux, 12 h (59%).

of substitution should make **PY** quadrupolar, which is linked to high  $\sigma^{(2)}$  values.<sup>1,12,14</sup> The obtained **PY** was characterized by <sup>1</sup>H and <sup>13</sup>C NMR, and high-resolution mass spectrometry (see ESI†). In addition, the solubility of **PY** in water was estimated to be  $\sim 2 \times 10^{-6}$  mol L<sup>-1</sup> (see Fig. S1 in the ESI†), which satisfied the essential requirement for living cell imaging without using excess organic solvents.<sup>5c</sup>

### One-photon absorption and fluorescence properties of PY

As mentioned above, **PY** has sufficient water solubility to stain living cells without the use of organic solvents. However, this water solubility is too low to reliably characterize the TP absorption. Therefore, all spectroscopic measurements were conducted using DMSO as the solvent, unless otherwise noted.

The one-photon absorption and fluorescence spectra of **PY** were recorded (Fig. 2). Interestingly, **PY** in DMSO exhibited an absorption peak at 510 nm, which is at a longer wavelength than those observed for **FLW**, **NP**, and **AC**.<sup>5c</sup> The anthracene-based dye, **AC**, has an absorption peak at a shorter wavelength (490 nm in DMSO), even though anthracene derivatives generally have longer absorption wavelengths than pyrene derivatives with similar substitution, as does the parent anthracene ( $\lambda_{\text{abs}} = 372$  nm compared with  $\lambda_{\text{abs}} = 330$  nm for pyrene in ethanol).<sup>11b</sup> A possible reason for this different behaviour is that the 1 and 6 positions of pyrene may accept stronger  $\pi$ -conjugation from the vinyl group-linked pyridinium moieties than the 2 and 6

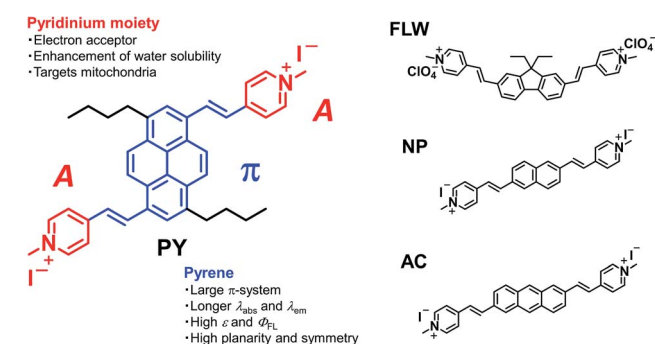


**Fig. 1** Molecular design of PAH-based A- $\pi$ -A dyes and the role of each moiety.

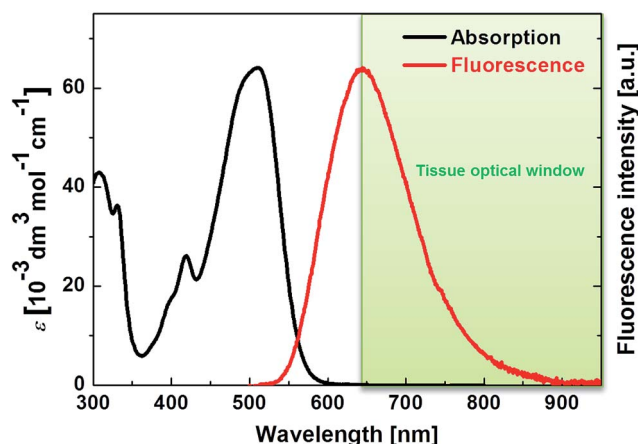


**Fig. 2** One-photon absorption and fluorescence spectra of **PY** in DMSO. The tissue optical window is indicated in green.





positions of anthracene.<sup>15</sup> As confirmed by DFT calculations, the substitution of acceptor groups at positions 1 and 6 in pyrene and at positions 9 and 10 in anthracene is most effective to induce red-shifted absorption spectra and to enhance the transition moments (Fig. S2 and S3†). On the other hand, it is expected that substitution at the 9 and 10 positions in anthracene by vinyl group-linked pyridinium moieties would result in a loss of planarity because of steric hindrance, which could decrease the  $\sigma^{(2)}$  value. Thus, pyrene has a structural advantage when compared with anthracene, as the pyrene  $\pi$ -system can be extended significantly without losing its planar structure. Importantly, the energy of a TP absorption allowed state is located at around one-half the energy level of a one-photon absorption allowed state; therefore, such a red-shifted one-photon absorption wavelength for **PY** is preferable for our purpose.

**PY** in DMSO showed a fluorescence peak at 650 nm, and the spectrum extended to 850 nm, which means that **PY** fluorescence is advantageously within the tissue optical window. Furthermore, a  $\Phi_{\text{FL}}$  value of 0.80 was measured; this value is significantly higher than those of the other PAH-based A- $\pi$ -A dyes (**FLW**, **NP**, and **AC** have  $\Phi_{\text{FL}}$  values in DMSO of 0.44, 0.36, and 0.66, at 542 nm, 516 nm, and 640 nm, respectively).<sup>5c</sup> The reason for the high  $\Phi_{\text{FL}}$  value of **PY** might be related to the above-mentioned stronger perturbation from  $\pi$ -conjugation with the pyrene chromophore or its rigid structure, which decreases vibrational deactivation.<sup>16</sup> The fluorescence peak of **PY** in aqueous solution was located at 650 nm. Thus, **PY** in water also fluoresced within the tissue optical window. The  $\Phi_{\text{FL}}$  value in aqueous solution was lower (0.10); highly polarized dyes exhibiting fluorescence at longer wavelengths tend to be less fluorescent in higher polarity solvents because of charge separation, which increases internal conversion.<sup>5c,17</sup> Considering that biological tissues and organs are usually less polar than water, such a strong decrease in the  $\Phi_{\text{FL}}$  value might be preferable to obtain background-free imaging.<sup>7d</sup> Thus, it was revealed that **PY** exhibits one-photon absorption that is suitable for realizing a longer wavelength TP absorption band and a fluorescence band with a high  $\Phi_{\text{FL}}$  value in the tissue optical window.

### Two-photon absorption properties of **PY**

The TP absorption spectrum of **PY** in DMSO was recorded using the open-aperture Z-scan technique.<sup>1</sup> The maximum  $\sigma^{(2)}$  value of **PY** was 1100 GM (1 GM =  $10^{-50}$  cm<sup>4</sup> per photon per molecule) at 950 nm (Fig. 3); this value is significantly higher than those for **FLW**, **NP**, and **AC**. **PY** also showed significant TP absorption at 1050 nm (380 GM), indicating that **PY** is compatible with the 1050 nm fibre laser source, whereas the TP absorption of **FLW**, **NP**, and **AC** at wavelengths longer than 1000 nm is quite small.<sup>5c</sup> These characteristics of **PY**, including the large  $\sigma^{(2)}$  value and longer TP absorption wavelength, might be explained by comparison with the other PAH-based A- $\pi$ -A dyes (e.g. **FLW**, **NP**, and **AC**, which show 740 GM at 780 nm, 712 GM at 695 nm, and 687 GM at 703 nm, respectively<sup>5c</sup>) as follows:

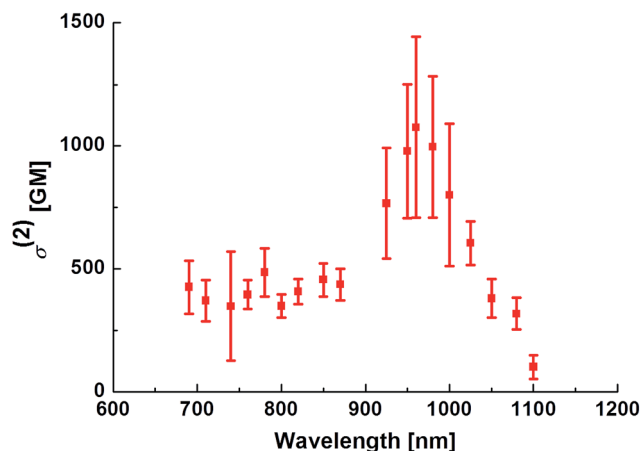


Fig. 3 Two-photon absorption spectrum of **PY** in DMSO.

1. Unlike **FLW**, **PY** has a quadrupolar structure, as do **NP** and **AC**.

2. **PY** has a larger  $\pi$ -electron system than the other PAH derivatives, especially **FLW** and **NP**.

3. **PY** is more strongly conjugated with the vinyl group-linked pyridinium moieties than **AC**, as mentioned in the section concerning one-photon absorption.

The performance of a TP active fluorescent molecule is generally estimated using the value of the TP action cross-section ( $\Phi\sigma^{(2)}$ ), which is the product of the values of  $\Phi_{\text{FL}}$  and  $\sigma^{(2)}$ . The  $\Phi\sigma^{(2)}$  value of **PY** at 950 nm was 880 GM; this value is quite large compared with the values for other TP active dyes, as described later (see Fig. 5).

### Imaging of living mitochondria with TPFM

To evaluate the actual performance of **PY** as a TP active fluorescent probe, the imaging of living mitochondria in Hek293 cells was carried out by TPFM. It is well-known that fluorophores possessing a pyridinium moiety can function as

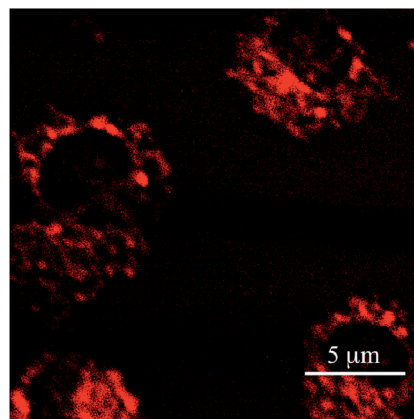
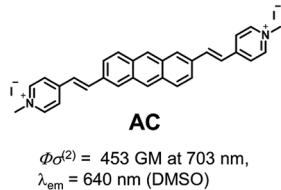
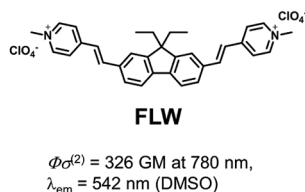
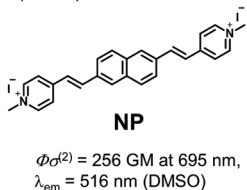
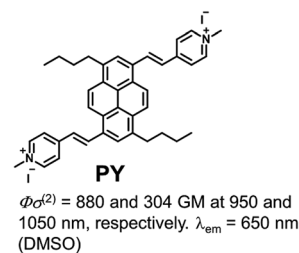
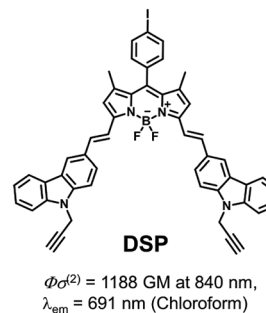


Fig. 4 Two-photon fluorescence microscope images of Hek293 cells stained with **PY**. This image was obtained with 950 nm excitation, and the fluorescence was collected through a 600–700 nm band-pass filter.



PAH-based A- $\pi$ -A dyes

## BODIPY-based dye



## Cyanine-based dyes

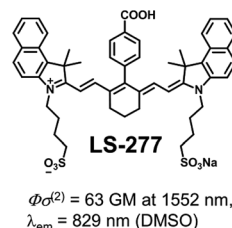
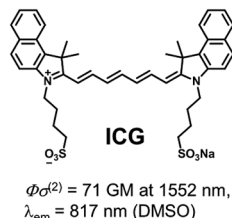
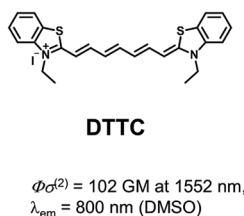
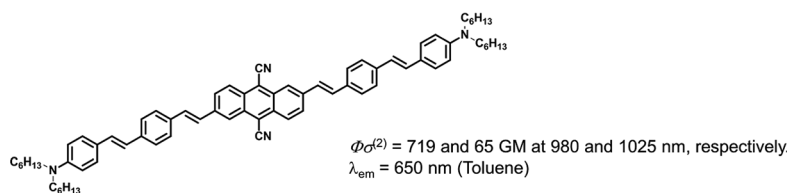
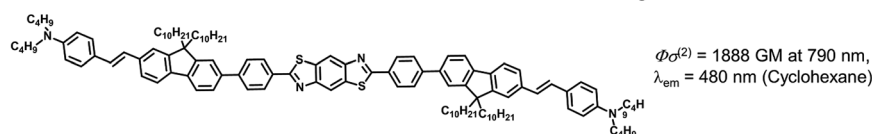
Anthracene-based  $\pi$ -extended dyeFluorene-based  $\pi$ -extended dye

Fig. 5 Examples of TP active fluorophores: PAH-based A- $\pi$ -A dyes,<sup>5c</sup> a BODIPY-based dye,<sup>5a</sup> cyanine-based dyes,<sup>5e</sup> an anthracene-based  $\pi$ -extended dye,<sup>1,21</sup> and fluorene-based  $\pi$ -extended dye.<sup>2,22</sup> These dyes were selected because they show attractive spectroscopic properties (TP absorption and fluorescence wavelengths, and  $\Phi\sigma^{(2)}$ ).

mitochondrial probes.<sup>5c,d,8</sup> A co-staining experiment with another mitochondrial probe (FLW)<sup>5d</sup> revealed that PY could also selectively accumulate on the mitochondria (Fig. S4†). As shown in Fig. 4, TPFM images of the mitochondria stained by PY were obtained with  $950$  nm excitation at a power of less than  $3$  mW. Considering that rhodamine 123,<sup>18</sup> a commercially available mitochondrial probe, requires a power of  $50$  mW in the same instruments, PY achieved extremely sensitive imaging, as expected from its high  $\Phi\sigma^{(2)}$  value. Importantly, the excitation power of a dye is proportional to the  $\Phi\sigma^{(2)}$  value. Therefore, if a TPFM that is equipped with an excitation light source operating at  $1050$  nm is available, TPFM imaging could be measured by

employing  $8.7$  mW of a  $1050$  nm light source. This power is sufficiently lower than the maximum output power of recent  $1050$  nm fibre lasers.<sup>9</sup> As the optical components of current TPFMs are not optimized for excitation at  $1050$  nm, it is not easy to obtain TPFM images with this excitation wavelength. However, after necessary optimization is realized, PY will be usable as a probe for TPFM employing the  $1050$  nm fibre laser.

## Comparison of PY with other dyes for TPFM

Finally, we compared PY with existing TP active dyes to demonstrate the superiority of our fluorophore (Fig. 5). As is apparent from the above discussion, PY has many desirable



properties for TPFM, such as a high  $\Phi\sigma^{(2)}$  value and longer TP absorption and fluorescence wavelengths, compared with other PAH-based A- $\pi$ -A dyes and commercially available mitochondrial dyes, such as green fluorescent protein (GFP;  $\Phi\sigma^{(2)} = 6$  GM at 800 nm and  $\lambda_{\text{em}} = 509$  nm)<sup>19</sup> and Rhodamine 123 ( $\Phi\sigma^{(2)} = 72$  GM at 800 nm and  $\lambda_{\text{em}} = 534$  nm).<sup>18</sup> There are a number of cyanine-based near infrared region (NIR) fluorescent dyes for TPFM that have recently been reported by Berezin and co-workers, such as ICG ( $\Phi\sigma^{(2)} = 71$  GM at 1500 nm and  $\lambda_{\text{em}} = 817$  nm) and LS-277 ( $\Phi\sigma^{(2)} = 63$  GM at 1500 nm and  $\lambda_{\text{em}} = 829$  nm).<sup>5e</sup> These dyes are highly attractive owing to their fluorescence within the tissue optical window and TP absorption activated by an ultrafast turnkey fibre laser source. However, these dyes are excited using 1500 nm light, which means their TP absorption bands are outside the tissue optical window. Furthermore, such dyes have relatively lower  $\Phi\sigma^{(2)}$  values at 1500 nm. Belfield *et al.* recently presented a large number of TP active fluorescent probes for bioimaging.<sup>2</sup> Although there are a few examples of dyes with  $\Phi\sigma^{(2)}$  values at their maximum TP absorption wavelength higher than that of **PY**, to the best of our knowledge, there are no dyes showing both TP absorption bands around 1000 nm and fluorescence bands within the optical tissue window that are more efficient than **PY**. In fact, most of the existing TP-active dyes can be excited in the short-wavelength NIR region around 700–800 nm rather than the so-called “second near-infrared window (NIR II, in the range 1000–1350 nm),” where it was recently proposed that the penetration of excitation light is ideal.<sup>20</sup> However, this means that these dyes are not compatible with a 1050 nm fibre laser even if they possess higher  $\Phi\sigma^{(2)}$  values than **PY**. As shown in Fig. 5, highly  $\pi$ -extended fluorene or anthracene derivatives, as well as BODIPY derivatives, exhibit relatively similar properties to **PY** with respect to  $\Phi\sigma^{(2)}$  values and fluorescence wavelengths, however, these dyes might not be suitable for bio-imaging due to their low solubility in water. In addition, the syntheses of these dyes are not trivial compared to that of **PY**. Thus, **PY** can be regarded as an exceptionally superior TP active dye with a comparatively simple and small structure. We emphasise that the outstanding properties of **PY** are strongly related to both the structural and electronic advantages of the pyrene chromophore, *i.e.* high planarity and symmetry, rigidness, synthetic accessibility for efficient  $\pi$ -extension and derivatization, and an underlying large  $\pi$ -system. Therefore, we believe that the strategic use of pyrene as a chromophore in TP active dyes will be of great importance and that **PY** itself can be further derivatized for other practical applications.

## Conclusions

We have developed a novel pyrene-based A- $\pi$ -A dye, **PY**, which showed a TP absorption band around 1000 nm and fluorescence in the tissue optical window with an outstanding  $\Phi\sigma^{(2)}$  value. Almost all the properties of **PY** are derived from the inherent structural and electronic advantages of the pyrene chromophore, including planarity, symmetry, rigidness, a large  $\pi$ -system, and synthetic accessibility for the efficient extension of  $\pi$ -conjugation. We have also demonstrated the ability of **PY**

to provide 3D images of the mitochondria in living Hek293 cells with higher sensitivity than the other PAH-based dyes and commercially available mitochondrial probes, as was expected from the performance of **PY** in spectroscopic measurements in solution. Finally, the comparison of **PY** with other known TP active fluorescent probes revealed that **PY** is an exceptional dye in terms of the location of its TP absorption around the NIR II window and its high  $\Phi\sigma^{(2)}$  value, indicating that **PY** is a promising candidate as a diagnostic tool and its ability to be used with the 1050 nm fibre laser will help the TPFM technique become more universal. To date, pyrene derivatives have been developed for many applications; therefore, there are a number of well-established synthetic methodologies where pyrene is used as a building block.<sup>23</sup> Thus, **PY** can be modified for many purposes, *e.g.* the further improvement of the compatibility of **PY** to the 1050 nm laser source by introducing other functional groups into the 3 and 8 positions on the pyrene chromophore, use of ligands for active targeting,<sup>24</sup> addition of environment sensitivity for the detection of chemical or biological events such as the generation of reactive oxygen species in mitochondria,<sup>8</sup> and further derivatization for building fluorescent nanoparticles.<sup>13</sup> Based on these facts and our findings, we believe that **PY** is a useful building block as a TP absorber and fluorophore for TPFM probes. In fact, we are currently focusing on the use of **PY** for not only *in vitro* cell imaging but also *in vivo* deep tissue imaging, using the 1050 nm fibre laser.

## Acknowledgements

We thank the JSPS Fellowship for Young Scientists (to Y. N.). This work was supported by a Grant-in-Aid for Scientific Research (no. 23350068) from the Ministry of Education, Culture, Sports, Science and Technology, Japan and Yamaguchi Prefecture Contracted R&D for the Industrial Cluster of Next Generation from Yamaguchi Prefectural Industrial Technology Institute, Japan.

## Notes and references

- 1 M. Pawlicki, H. A. Collins, R. G. Denning and H. L. Anderson, *Angew. Chem., Int. Ed.*, 2009, **48**, 3244–3266.
- 2 S. Yao and K. D. Belfield, *Eur. J. Org. Chem.*, 2012, **17**, 3199–3217.
- 3 W. Denk, J. H. Strickler and W. W. Webb, *Science*, 1990, **248**, 73–76.
- 4 (a) R. Weissleder, *Nat. Biotechnol.*, 2001, **19**, 316–317; (b) Y. Pu, L. Shi, S. Pratavieira and R. R. Alfano, *J. Appl. Phys.*, 2013, **114**, 153102.
- 5 (a) X. Zhang, Y. Xiao, J. Qi, J. Qu, B. Kim, X. Yue and K. D. Belfield, *J. Org. Chem.*, 2013, **78**, 9153–9160; (b) T. Zhang, X. Zhu, C. C. W. Cheng, W.-M. Kwok, H.-L. Tam, J. Hao, D. W. J. Kwong, W.-K. Wong and K.-L. Wong, *J. Am. Chem. Soc.*, 2011, **133**, 20120–20122; (c) M. Tominaga, S. Mochida, H. Sugihara, K. Satomi, H. Moritomo, A. Fuji, A. Tomoyuki, Y. Suzuki and J. Kawamata, *Chem. Lett.*, 2014, in press; (d) S. Tani, K. Nakagawa, T. Honda, H. Saito, Y. Suzuki, J. Kawamata, M. Uchida, A. Sasaki and M. Kinjo,



- Curr. Pharm. Biotechnol.*, 2012, **13**, 2649–2654; (e) M. Y. Berezin, C. Zhan, H. Lee, C. Joo, W. J. Akers, S. Yazdanfar and S. Achilefu, *J. Phys. Chem. B*, 2011, **115**, 11530–11535.
- 6 (a) Y.-C. Zheng, M.-L. Zheng, S. Chen, Z.-S. Zhao and X.-M. Duan, *J. Mater. Chem. B*, 2014, **2**, 2301–2310; (b) H. Zhang, J. Fan, H. Dong, S. Zhang, W. Xu, J. Wang, P. Gao and X. Peng, *J. Mater. Chem. B*, 2013, **1**, 5450–5455; (c) N. Xie, K. Feng, B. Chen, M. Zhao, S. Peng, L.-P. Zhang, C.-H. Tung and L.-Z. Wu, *J. Mater. Chem. B*, 2014, **2**, 502–510; (d) X. Wang, J. Sun, W. Zhang, X. Ma, J. Lv and B. Tang, *Chem. Sci.*, 2013, **4**, 2551–2556; (e) K. P. Divya, S. Sreejith, P. Ashokkumar, K. Yuzhan, Q. Peng, S. K. Maji, Y. Tong, H. Yu, Y. Zhao, P. Ramamurthy and A. Ajayaghosh, *Chem. Sci.*, 2014, DOI: 10.1039/c4sc00736k; (f) G. Masanta, C. H. Heo, C. S. Lim, S. K. Bae, B. R. Cho and H. M. Kim, *Chem. Commun.*, 2012, **48**, 3518–3520; (g) E. De Meulenaere, W.-Q. Chen, S. Van Cleuvenbergen, M.-L. Zheng, S. Psilodimitrakopoulos, R. Paesen, J.-M. Taymans, M. Ameloot, J. Vanderleyden, P. Loza-Alvarez, X.-M. Duan and K. Clays, *Chem. Sci.*, 2012, **3**, 984–995; (h) J. Jing, J.-J. Chen, Y. Hai, J. Zhan, P. Xu and J.-L. Zhang, *Chem. Sci.*, 2012, **3**, 3315–3320; (i) J. Massin, A. Charaf-Eddin, F. Appaix, Y. Bretonnière, D. Jacquemin, B. van der Sanden, C. Monnereau and C. Andraud, *Chem. Sci.*, 2013, **4**, 2833–2843; (j) P. Yan, A. Xie, M. Wei and L. M. Loew, *J. Org. Chem.*, 2008, **73**, 6587–6594; (k) P. Yan, C. D. Acker, W.-L. Zhou, P. Lee, C. Bollensdorff, A. Negrean, J. Lotti, L. Sacconi, S. D. Antic, P. Kohl, H. D. Mansvelder, F. S. Pavone and L. M. Loew, *Proc. Natl. Acad. Sci. U. S. A.*, 2012, **109**, 20443–20448; (l) J. Massin, A. Charaf-Eddin, F. Appaix, Y. Bretonnière, D. Jacquemin, B. van der Sanden, C. Monnereau and C. Andraud, *Chem. Sci.*, 2013, **4**, 2833–2843.
- 7 (a) Z. Yang, J. Cao, Y. He, J. H. Yang, T. Kim, X. Peng and J. S. Kim, *Chem. Soc. Rev.*, 2014, **43**, 4563–4601; (b) A. P. de Silva, H. Q. N. Gunaratne, T. Gunnlaugsson, A. J. M. Huxley, C. P. McCoy, J. T. Rademacher and T. E. Rice, *Chem. Rev.*, 1997, **97**, 1515–1566; (c) R. W. Sinkeldam, N. J. Greco and Y. Tor, *Chem. Rev.*, 2010, **110**, 2579–2619; (d) A. S. Klymchenko and R. Kreder, *Chem. Biol.*, 2014, **21**, 97–113.
- 8 (a) J.-T. Hou, M.-Y. Wu, K. Li, J. Yang, K.-K. Yu, Y.-M. Xie and X.-Q. Yu, *Chem. Commun.*, 2014, **50**, 8640–8643; (b) P. Li, H. Xiao, Y. Cheng, W. Zhang, F. Huang, W. Zhang, H. Wang and B. Tang, *Chem. Commun.*, 2014, **50**, 7184–7187; (c) S. Hirose, S. Arai and S. Takeoka, *Chem. Commun.*, 2012, **48**, 4845–4847; (d) N. Jiang, J. Fan, T. Liu, J. Cao, B. Qiao, J. Wang, P. Gao and X. Peng, *Chem. Commun.*, 2013, **49**, 10620–10622.
- 9 Examples of 1050 nm femtosecond fibre laser; Ytterbium-1100 (Tekhnoscan), FCPA MicroJewel (IMRA), Origami (Onefive) or Fidelity (Coherent), and so on.
- 10 (a) S. Keereweere, J. D. Kerrebijn, P. B. van Driel, B. Xie, E. L. Kaijzel, T. J. Snoeks, I. Que, M. Hutteman, J. R. van der Vorst, J. S. Mieog, A. L. Vahrmeijer, C. J. van de Velde, R. J. Baatenburg de Jong and C. W. Lowik, *Mol. Imag. Biol.*, 2011, **13**, 199–207; (b) K. Licha and C. Olbrich, *Adv. Drug Delivery Rev.*, 2005, **57**, 1087–1108; (c) J. Rao, A. Dragulescu-Andrasi and H. Yao, *Curr. Opin. Biotechnol.*, 2007, **18**, 17–25.
- 11 (a) S. Dufresne, I. U. Roche, T. Skalski and W. G. Skene, *J. Phys. Chem. C*, 2010, **114**, 13106–13112; (b) Y. Niko, Y. Hiroshige, S. Kawauchi and G. Konishi, *J. Org. Chem.*, 2012, **77**, 3986–3996.
- 12 H. M. Kim, Y. O. Lee, C. S. Lim, J. S. Kim and B. R. Cho, *J. Org. Chem.*, 2008, **73**, 5127–5130.
- 13 (a) K. Li, W. Qin, D. Ding, N. Tomczak, J. Geng, R. Liu, J. Liu, X. Zhang, H. Liu, B. Liu and B. Z. Tang, *Sci. Rep.*, 2013, **3**, 1150, DOI: 10.1038/srep0115; (b) A. S. Klymchenko, E. Roger, N. Anton, H. Anton, I. Shulov, J. Vermot, Y. Mély and T. F. Vandamme, *RSC Adv.*, 2012, **2**, 11876–11886; (c) J. H. Kim, S. Lee, K. Park, H. Y. Nam, S. Y. Jang, I. Youn, K. Kim, H. Jeon, R. W. Park, I. S. Kim, K. Choi and I. C. Kwon, *Angew. Chem., Int. Ed.*, 2007, **46**, 5779–5782; (d) A. Reisch, P. Didier, L. Richert, S. Oncul, Y. Arntz, Y. Mély and A. S. Klymchenko, *Nat. Commun.*, 2014, **5**, DOI: 10.1038/ncomms5089.
- 14 M. Albota, D. Beljonne, J.-L. Brédas, J. E. Ehrlich, J.-Y. Fu, A. A. Heikal, S. E. Hess, T. Kogej, M. D. Levin, S. R. Marder, D. McCord-Maughon, J. W. Perry, H. Röckel, M. Rumi, G. Subramaniam, W. W. Webb, X.-L. Wu and C. Xu, *Science*, 1998, **281**, 1653–1656.
- 15 (a) S. Méry, D. Haristoy, J.-F. Nicoud, D. Guillon, H. Monobe and Y. Shimizu, *J. Mater. Chem.*, 2003, **13**, 1622–1630; (b) M. Uchimura, Y. Watanabe, F. Araoka, J. Watanabe, H. Takezoe and G. Konishi, *Adv. Mater.*, 2010, **22**, 4473–4478; (c) Y. Niko and G. Konishi, *J. Synth. Org. Chem., Jpn.*, 2012, **70**, 918–927.
- 16 N. J. Turro, V. Ramamurthy and J. C. Scaiano, *Modern Molecular Photochemistry of Organic Molecules*, University Science Books, Sausalito, California, 2010, pp. 289–290.
- 17 (a) N. J. Turro, V. Ramamurthy and J. C. Scaiano, *Modern Molecular Photochemistry of Organic Molecules*, University Science Books, Sausalito, California, 2010, pp. 261–303; (b) T. Soujanya, R. W. Fessenden and A. Samanta, *J. Phys. Chem.*, 1996, **100**, 3507–3512; (c) G. F. Mes, B. De Jong, H. J. Van Ramesdonk, J. W. Verhoeven, J. M. Warman, M. P. De Haas and L. E. W. Horsman-van den Dool, *J. Am. Chem. Soc.*, 1984, **106**, 6524–6528.
- 18 R. Wolleschensky, T. Feurer, R. Sauerbrey and U. Simon, *Appl. Phys. B*, 1998, **67**, 87–94.
- 19 P. T. C. So, C. Y. Dong, B. R. Masters and K. M. Berland, *Annu. Rev. Biomed. Eng.*, 2000, **2**, 399–429.
- 20 (a) R. Subha, V. Nalla, J. H. Yu, S. W. Jun, K. Shin, T. Hyeon, C. Vijayan and W. Ji, *J. Phys. Chem. C*, 2013, **117**, 20905–20911; (b) J. T. Robinson, G. Hong, Y. Liang, B. Zhang, O. K. Yaghi and H. Dai, *J. Am. Chem. Soc.*, 2012, **134**, 10664–10669; (c) G. Hong, J. C. Lee, J. T. Robinson, U. Raaz, L. Xie, N. F. Huang, J. P. Cooke and H. Dai, *Nat. Med.*, 2012, **18**, 1841–1846.
- 21 S. K. Lee, W. J. Yang, J. J. Choi, C. H. Kim, S.-J. Jeon and B. R. Cho, *Org. Lett.*, 2005, **7**, 323–326.



- 22 S. Yao, H.-Y. Ahn, X. Wang, J. Fu, E. W. van Stryland, D. J. Hagan and K. D. Belfield, *J. Org. Chem.*, 2010, **75**, 3965–3974.
- 23 (a) T. M. Figueira-Duarte and K. Müllen, *Chem. Rev.*, 2011, **111**, 7260–7314; (b) Y. Niko, S. Kawauchi, S. Otsu, K. Tokumaru and G. Konishi, *J. Org. Chem.*, 2013, **78**, 3196–3207; (c) Y. Niko, S. Kawauchi and G. Konishi, *Chem.–Eur. J.*, 2013, **19**, 9760–9765; (d) Y. Niko, S. Sasaki, S. Kawauchi, K. Tokumaru and G. Konishi, *Chem.–Asian J.*, 2014, **9**, 1797–1807; (e) Y. Niko, Y. Cho, S. Kawauchi and G. Konishi, *RSC Adv.*, 2014, **4**, 36480–36484.
- 24 S. Luo, E. Zhang, Y. Su, T. Cheng and C. Shi, *Biomaterials*, 2011, **32**, 7127–7138.

